VOLATILE ORGANIC COMPOUNDS IN EXHALED BREATH: REAL-TIME MEASUREMENTS, MODELING, AND BIO-MONITORING APPLICATIONS

Julian King[a,c], Karl Unterkofler[b,c], Susanne Teschl[d], Anton Amann[c], Gerald Teschl[a]

[a]Faculty of Mathematics, University of Vienna, Nordbergstr. 15, A-1090 Wien, Austria
[b]Vorarlberg University of Applied Sciences, Hochschulstr. 1, A-6850 Dornbirn, Austria
[c]Breath Research Institute, Austrian Academy of Sciences, Rathausplatz 4, A-6850 Dornbirn, Austria
[d]University of Applied Sciences Technikum Wien, Höchstädtplatz 5, A-1200 Wien, Austria

[a]Julian.King@univie.ac.at; Gerald.Teschl@univie.ac.at, [b]Karl.Unterkofler@fhv.at,
[c]Anton.Amann@oeaw.ac.at. [d]Susanne.Teschl@technikum-wien.at

ABSTRACT

The present paper reviews some paradigmatic applications of modeling and simulation in the context of exhaled breath analysis, which has emerged as a promising tool for collecting *non-invasive* and *continuous* information on the metabolic and physiological state of an individual. In particular, it is illustrated how real-time breath profiles of volatile organic compounds (as obtained, e.g., by PTR-(TOF)-MS) can be used to extract *in vivo* estimates of endogenous quantities that are difficult to access by conventional analytical approaches based on blood, urine, or tissue. Typical examples include the determination of production and metabolism rates, as well as tracking the tissue accumulation of exogenously administered trace gases (e.g., volatile anesthetics).

Keywords: exhaled breath analysis, volatile organic compounds (VOCs), physiological modeling, pulmonary gas exchange

1. INTRODUCTION

Due to its broad scope and applicability, breath gas analysis holds great promise as a versatile framework for general bio-monitoring applications (Amann and Smith 2005).

Volatile organic compounds (VOCs) in exhaled breath represent a unique biochemical probe in the sense that they can provide both *non-invasive* and *continuous* information on the metabolic and physiological state of an individual. Apart from diagnostics and therapy control, this information might fruitfully be used for dynamic assessments of normal physiological function (e.g., during exercise stress tests, in an intra-operative setting, or in a sleep lab (King *et al.* 2009; Schubert *et al.* 2012; King *et al.* 2012a)), pharmacodynamics (drug testing (Beauchamp *et al.* 2010)), or for quantifying body burden in response to environmental exposure (e.g., in occupational health).

However, quantitative modeling approaches for exploiting this potential remain challenging due to the multifaceted impact of physiological parameters (such as cardiac output or breathing patterns) as well as due to the sparse and often conflicting data regarding potential biochemical sources or sinks of VOCs in the human body. Within this framework, a primary goal of our investigations is to clarify the behavior of several prototypic breath trace gases by providing phenomenological reference data as well as mechanistic modeling. The present paper reviews some paradigmatic applications in this context, discussing models for the endogenous VOC isoprene (a tentative biomarker for oxidative stress and lipid metabolism disorders) and the exogenously administered volatile anesthetic agent sevoflurane.

2. EXPERIMENTAL METHODS

The range of measurement techniques employed for breath gas analytical investigations is extremely diverse and each method comes with its specific strengths and weaknesses. Here, the main focus is on direct mass spectrometry, particularly proton transfer reaction mass spectrometry (PTR-MS) (Lindinger *et al.* 1998). A major hallmark of PTR-MS is its *real-time* capability, allowing for concentration measurements of VOCs with a sampling frequency of more than 1 Hz (i.e., on a breath-by-breath resolution).

The possibility of generating high frequency data can be viewed as an essential requirement for relating short-term variations of breath VOC concentrations to quick metabolic and physiological changes (e.g., in blood or ventilatory flow). An experimental setup for the parallel recording of real-time PTR-MS trace gas profiles as well as hemodynamic and respiratory parameters is shown in Figure 1 (King *et al.* 2009; King *et al.* 2010b).

This instrumentation provides an excellent opportunity to model/simulate the blood-gas kinetics and systemic distribution of specific VOCs within the human body, and to validate such simulations by adequately designed experimental regimes, e.g., by measuring concentration levels during workload segments on an ergometer (see Figure 1) or by looking at the concentration changes during sleep (with different sleep-related events giving rise to different VOC breath patterns (King *et al.* 2012a)).

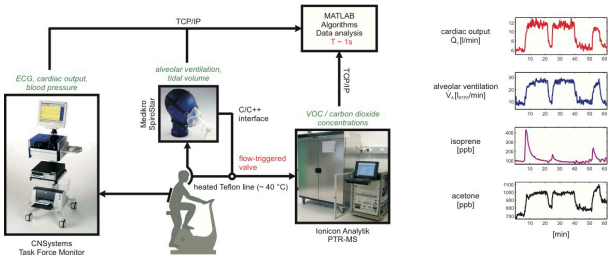

Figure 1: Experimental setup used for obtaining VOC profiles in conjunction with a number of physiological parameters. Items in italic correspond to measurable variables. Right panel: typical smoothed profiles of *end-tidal* isoprene and acetone concentrations in response to the following workload regime: 7 min resting, 15 min ergometer challenge at 75 Watts, 3 min resting, 15 min at 75 Watts, 12 min resting, 5 min at 75 Watts, 5 min resting. Data correspond to one single volunteer.

3. MODELING BREATH VOC PROFILES

In classical pulmonary inert gas elimination theory the relationship between the blood concentrations of VOCs and their respective concentrations in the gaseous phase is captured by the well-known equation due to Farhi (1967), viz.,

$$C_{\text{measured}} = C_{\text{A}} = \lambda_{\text{b:air}}\, C_{\text{a}} = \frac{C_{\text{v}}}{\lambda_{\text{b:air}} + \dot{V}_{\text{A}} / \dot{Q}_{\text{c}}} \qquad (1)$$

where the subscripts A, a, and v denote alveolar, arterial, and mixed-venous concentrations, respectively, and λ is the substance-specific blood:air partition coefficient describing the diffusion equilibrium at the alveolar-capillary interface according to Henry's law. The influence of respiratory and hemodynamic variables is captured by the ratio between alveolar ventilation $\dot{V}_A$ and cardiac output $\dot{Q}_c$.

3.1. Isoprene modeling

While the Farhi equation represents the starting point for any quantitative modeling approach in exhaled breath analysis, it turns out that this simple formulation is generally inadequate for explaining the observed dynamic behavior of breath VOCs in response to relatively quick physiological transitions.

Indeed, as can be seen in Figure 1 the profiles of isoprene and acetone considerably depart from the trend predicted by Equation (1). More specifically, at the onset of exercise the ventilation-perfusion ratio increases drastically and hence, other factors being equal, a more or less pronounced drop in the respective breath concentrations could be expected (such a drop can in fact be observed for some endogenous breath VOCs, e.g., butane and methane, see (King *et al.* 2010b) and Figure 6, respectively). As we shall illustrate in the following, in the case of isoprene this discrepancy can be explained by reference to a peripheral (extra-hepatic) production of the compound, which is realized by complementing the basic Farhi model with two systemic compartments, affecting the time evolution of the mixed-venous concentration according to their fractional perfusion.

To this end, it is instructive to note that exercise bouts at constant workload interrupted by breaks of variable duration lead to markedly different heights of the characteristic breath isoprene concentration peak at the onset of pedaling, despite an almost identical behavior of cardiac output and alveolar ventilation throughout all workload segments (see Figure 1). This appears to exclude pulmonary gas exchange as a primary cause for the peak-shaped dynamics and points towards a substance-specific wash-out from an isoprene buffer tissue within the human body. In order to further investigate this hypothesis we additionally performed a series of *one-legged* ergometer experiments, showing that a switch of the working leg after a short break following an ergometer exercise segment results in an immediate recovery of the initial peak height, whereas continuing the exercise with the same leg leads to a wash-out effect similar to the two-legged case (King *et al.* 2010a).

From the phenomenological findings outlined above we concluded that a major part of isoprene variability during exercise phases can be ascribed to an increased fractional perfusion of the working skeletal muscles, eventually leading to higher isoprene levels in mixed venous blood at the onset of physical activity. This idea has subsequently been incorporated into a physiologically based compartment model (King *et al.* 2010a; Koc *et al.* 2011), describing the distribution of isoprene in various functional units of the organism, see Figure 2. By writing down the mass balance relations for each compartment such model structures can directly be expressed as a set of ordinary differential equations with smooth right hand side **g**,

$$\dot{\mathbf{x}}(t) = \mathbf{g}(\mathbf{x}(t), \mathbf{u}(t), \boldsymbol{\theta}), \quad \mathbf{x}(t_0) = \mathbf{x}_0 \qquad (2)$$

where the state vector **x** contains the molecular concentrations of the investigated trace gas within the tissue compartments introduced; **u** stands for external inputs (blood/respiratory flows, temperature, etc.) that can be modified by experimentation; $\boldsymbol{\theta}$ lumps together an ensemble of constant, unknown model parameters (including, e.g., kinetic constants such as endogenous production or metabolization rates). The latter have to be estimated from the available process data (possibly together with some components of the initial conditions $\mathbf{x}_0$), which are linked to the system dynamics via the scalar *measurement equation*

$$y(t) = h(\mathbf{x}(t), \boldsymbol{\theta}). \qquad (3)$$

Here, h is some smooth function defining the observable model output (i.e., the measurable breath concentration).

The proposed model can be calibrated based on the physiological data derived from the setup in Figure 1.

More specifically, the unknown (and volunteer-specific) model parameters and initial equilibrium concentrations are determined by standard least-squares procedures, implementing a *multiple shooting* routine in Matlab.

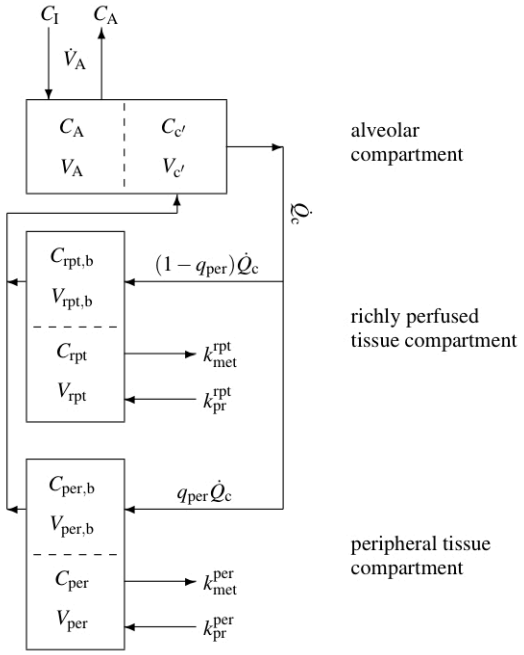

Figure 2: Schematic representation of the model structure used for describing the dynamics of isoprene concentrations in various parts of the human body. The latter is divided into three distinct functional units: alveolar/end-capillary compartment (gas exchange), richly perfused tissue (metabolism and production) and peripheral (muscle) tissue (storage, metabolism and production). Fractional blood flow to the periphery is denoted by q_{per}, while k_{pr} and k_{met} represent constant production and (linear) metabolism rates, respectively. Dashed boundaries indicate a diffusion equilibrium as determined by the respective blood:air and blood:tissue partition coefficients. Subscripts denote as follows: I-inhaled; A-alveolar; c'-end-capillary; rpt-richly perfused tissue; per-peripheral tissue; b-blood.

This iterative method can be seen as a generalization of the Gauss–Newton algorithm, designed to avoid divergence issues of the latter due to large residuals. For further details as well as convergence and stability properties we refer to (Peifer and Timmer 2007) and references therein. Figure 3 summarizes the results of these calculations.

The physiological mechanism revealed by this simulation is as follows: at rest the peripheral (muscle) compartment is characterized by high isoprene concentrations resulting from extra-hepatic production at a constant rate. However, due to the relatively small fractional perfusion of these tissues, the mixed venous concentration is mainly governed by the lower isoprene content of the venous blood returning from the richly perfused tissue group. At the start of exercise, the fractional perfusion q_{per} to the periphery drastically increases. Consequently, isoprene is washed out from the peripheral compartment and the mixed venous concentration becomes dominated by peripheral venous return. The isoprene concentration peak visible in breath can thus be interpreted as a direct consequence of the associated rise in mixed venous blood concentrations.

Two important findings emerge from this modeling analysis. Firstly, it is suggested that the working skeletal muscles act as an active production site of isoprene in the human body. While such a hypothesis contrasts previous work postulating a purely hepatic origin of this compound, recent investigations observing a pronounced reduction of breath and blood isoprene levels in late stage Duchenne muscle dystrophy patients support this novel viewpoint (King *et al.* 2012b). In particular, the latter study is a good example how mechanistic modeling ultimately allows for designing theory-driven experiments.

Furthermore, the proposed model can serve as a quantitative tool for estimating relevant endogenous parameters governing isoprene dynamics (such as production or metabolism rates) on the basis of exhaled breath, hence allowing for the non-invasive extraction of patient-specific metabolic information. Indeed, the relative standard deviations of the estimated parameters as determined by *residual bootstrapping* usually range below 10%, thus demonstrating that the unknown model quantities are reasonably identifiable within the present experimental scenario (King *et al.* 2010a).

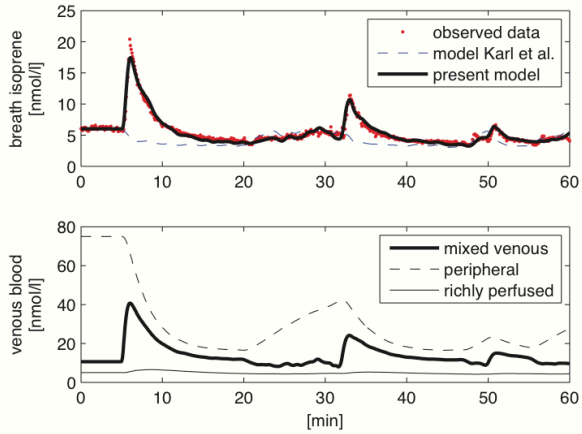

Figure 3: First panel: simulation of individual breath isoprene behavior during exercise conditions, compare Figure 1; second panel: predicted concentrations in mixed venous blood and venous blood returning from the peripheral (muscle) and richly perfused tissue groups.

3.2. Anesthetic monitoring

It has recently been demonstrated that PTR-MS allows for acquiring breath concentration profiles of inhalational (e.g., sevoflurane) as well as intravenous (e.g., propofol) anesthetic agents in real-time. By coupling these profiles with physiological modeling concepts and signal processing tools, non-invasive *on-line* schemes for continuously monitoring certain key quantities during anesthesia might be derived. Examples

include the estimation of agent concentrations in blood or the central nervous system (i.e., the target sites), or tracking major hemodynamic variables such as cardiac output.

For this purpose, a simple compartmental description for capturing the tissue accumulation of sevoflurane during inhalation anesthesia has been developed (King *et al.* 2011b). The model is largely analogous to the one in Figure 2, except that a brain compartment has been added and the peripheral tissue compartment has been replaced by adipose tissue, which represents a large storage volume for lipophilic compounds such as sevoflurane. Additionally, due to the fact that sevoflurane is not produced endogenously and only poorly metabolized, all production and metabolism rates have been set to zero. Using standard literature values for the involved physiological parameters, the resulting model predictions are in good agreement with published *in vivo* concentration profiles, see Figure 4.

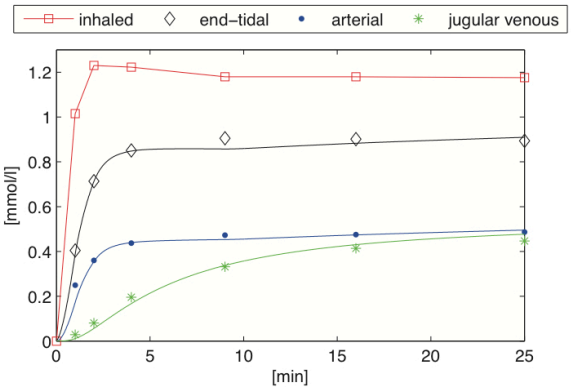

Figure 4: Simulation of sevoflurane profiles in inspired/ end-tidal air, arterial blood, and jugular venous blood during administration of approx. 3% sevoflurane over 25 min. Discrete points reflect sample means associated with pooled data from 11 patients as measured by Nakamura *et al*. (1999).

Going beyond the direct problem of simulating the time evolution of breath sevoflurane levels given a number of physiological parameters, it is intriguing to ask whether one can also solve the related inverse problem, e.g., whether one can reconstruct (possibly in real-time) physiological quantities such as cardiac output or tissue (particularly brain) sevoflurane concentrations on the basis of sevoflurane dynamics observed in exhaled breath. Note, that this represents a question of considerable clinical relevance, as the former quantities are reflective of both the patient's hemodynamic status as well as his anesthetic/amnestic response, however, they are not easily accessible during the perioperative period. In the following we will present a proof-of-concept how the problem stated above can be approached by employing nonlinear filtering techniques. The limiting factor here is that due to the lack of adequate *in vivo* data the reconstruction is based on *simulated* rather than measured breath sevoflurane data.

In a first step, by employing zero-order hold sampling and introducing Gaussian, white, zero-mean noise sequences $\mathbf{w}_k$, ϑ_k, and v_k the sevoflurane dynamics given by Equations (2) and (3) can be discretized as

$$\mathbf{x}_k = G_{k-1}\left(\theta_{k-1}\right)\mathbf{x}_{k-1} + \mathbf{f}_{k-1} + \mathbf{w}_{k-1}$$
$$\theta_k = \theta_{k-1} + \vartheta_{k-1}$$
$$y_k = H_k\mathbf{x}_k + d_k + v_k$$

Here, the time-varying parameter θ reflects cardiac output and y_k is the measurable breath sevoflurane concentration. The aim is to sequentially reconstruct $\mathbf{x}$ (i.e., the non-accessible compartmental concentrations) and θ from the stacked observations $Y_k = (y_k,\ldots,y_1)$, which in this case, as mentioned before, have been generated by simulating the original deterministic system (2) and (3) and adding Gaussian noise with fixed variance).

Sequential state and parameter reconstruction can be achieved by virtue of a marginalized particle filtering scheme as introduced in (Schön *et al.* 2005). Briefly, starting from Gaussian prior densities $p(\mathbf{x}_0)$ and $p(\theta_0)$ encapsulating the available information on the initial compartment concentrations and the initial cardiac output, respectively, this framework allows for the recursive approximation of the posterior probability $p(\mathbf{x}_k, \Theta_k \,|\, Y_k)$, which embodies all accessible information on $\mathbf{x}_k$ and the parameter sequence $\Theta_k = (\theta_k,\ldots,\theta_0)$ up to time k. For the purpose of computing this density, it is instructive to note that, conditional on Θ_k, the discretized equations above represent a linear Gaussian system. Consequently, we may decompose

$$p(\mathbf{x}_k,\Theta_k \,|\, Y_k) = p(\mathbf{x}_k \,|\, \Theta_k, Y_k)\,p(\Theta_k \,|\, Y_k) \qquad (4)$$

where the first factor can be determined analytically by means of the standard Kalman filter formulae. Simultaneously, particle filtering is employed for producing m samples (particle trajectories) $\Theta_{k,i} = (\theta_{k,i},\ldots,\theta_{0,i})$, $i = 1,\ldots,m$ following $p(\Theta_k|Y_k)$, thus allowing for a (point mass) approximation of the second factor in Equation (4).

Combining these two mechanisms we end up with a bank of m Kalman filters running in parallel, each one associated with a single particle trajectory $\Theta_{k,i}$. When proceeding from time k-1 to time k, first the time update of each Kalman filter is performed. The resulting *a priori* estimates are subsequently used to update each particle trajectory according to the standard *sampling importance resampling* scheme fundamental to particle filtering (Gordon *et al.* 1993). In a last step, the measurement update for each Kalman filter is performed using the previously updated particle trajectory. Finally, the arithmetic mean of all *a posteriori* estimates (conditional means) derived from

the m separate Kalman filters constitutes a minimum mean square error estimate of the compartment concentrations $\mathbf{x}_k$, and similarly for θ_k. For further technical details the interested reader is referred to (King *et al.* 2011b).

The applicability of this filtering scheme within the anesthetic monitoring framework introduced above is demonstrated in Figure 5. Here, the mean and standard deviation of the prior distribution $p(\theta_0)$ reflecting the initial knowledge about the current cardiac output is set to 8 L/min and 3 L/min, respectively (corresponding to a poor initial guess with relatively large uncertainty). The resulting state and parameter estimates calculated as described above provide a reasonable reconstruction of their simulated counterparts. In particular, incidences such as abrupt drops in cardiac output are recognized within a delay time that is sufficiently small for enabling intra-operative interventions.

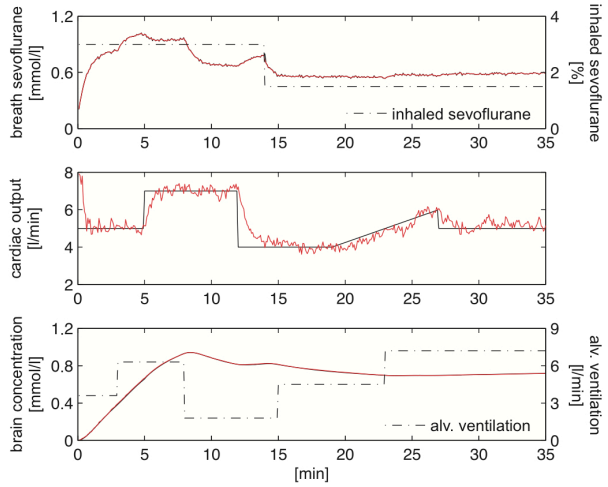

Figure 5: Simulated (solid black lines) and recovered (solid red lines) profiles of the breath sevoflurane concentration, cardiac output and brain concentration, using a marginalized particle filter with size m = 300. Dash-dotted lines represent the profiles of the inhaled sevoflurane concentration and alveolar ventilation used for the simulation of breath sevoflurane data.

4. OUTLOOK AND CONCLUSIONS

While the above approaches demonstrate that coupling the high-frequency information obtainable from breath gas analytical techniques with well-established tools from parameter identification and signal processing potentially allows for (continuous) estimation and monitoring of endogenous processes, we are well aware of the fact that several aspects have to be investigated more deeply before such methodologies can become clinically relevant (e.g., as a part of automated anesthesia delivery systems in the case of sevoflurane).

The primary building block for a successful implementation is the availability of reliable physiological models for the endogenous distribution of the volatile compounds under study. Consequently, additional experimental efforts, data gathering and modeling attempts (accounting for potential substance-specific confounding factors, e.g., time-varying metabolization patterns, compartmental sequestration, etc.) are required in order to extend the validity of simple models such as the ones presented above over a sufficiently wide range of possible dynamics.

Another important contribution towards generalizing such modeling results is the increased availability of analytical techniques allowing for *parallel* real-time measurements of distinct substance classes within the same experimental regime. A prototypic method in this regard time-of-flight mass spectrometry coupled with chemical ionization, as realized for instance in PTR-TOF (Herbig *et al.* 2009). Briefly, such devices obviate the usual trade-off between sampling frequency and the number of trace gases that can be monitored simultaneously and offer very detailed spectral information in every sampling instant. Typical results are shown in Figure 6.

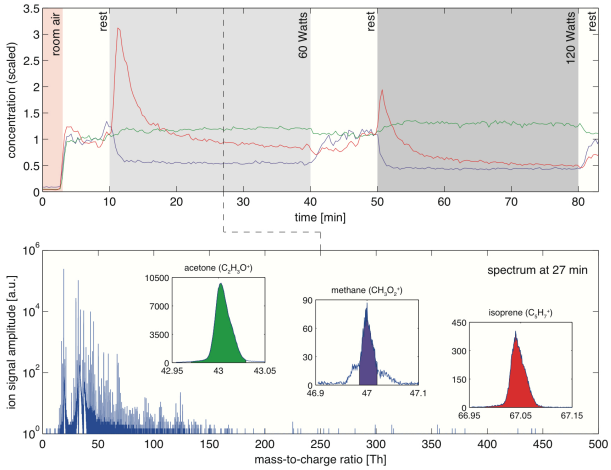

Figure 6: Profiles of breath acetone, methane, isoprene during a similar exercise scenario as in Figure 1. Data correspond to one single volunteer and are obtained by chemical ionization TOF mass spectrometry using O_2^+ primary ions. The second panel shows the TOF spectrum at 27 min. In the ideal (non-overlapping) case, each peak in the spectrum corresponds to one VOC, which may be identified *a priori* using pure gas standards. The concentration at a specific time instant is roughly proportional to the associated area under curve. Note that distinct VOCs can show a rather different behavior in response to the same physiological stimulus. While methane obeys the dynamics predicted by Equation (1), substance-specific factors like peripheral wash-out (isoprene) or airway gas exchange (acetone, cf. (King *et al.* 2012c; King *et al.* 2011a)) may lead to characteristic deviations from that trend.

As a concluding remark, the development of quantitative formulations relating breath concentrations of trace gases to their underlying systemic levels clearly lags behind the enormous analytical progress in exhaled breath analysis. In this sense, the approaches presented in this paper are also intended to further strengthen the

role of mathematical modeling and simulation as core techniques in breath gas analytical investigations.

ACKNOWLEDGMENTS

J.K., K.U., and G.T. gratefully acknowledge support from the Austrian Science Fund (FWF) under Grant No. Y330 and Grant No. P24736-B23. We appreciate the generous support of the government of Vorarlberg, Austria.

REFERENCES

Amann, A., Smith, D., (eds.), 2005. *Breath Analysis for Clinical Diagnosis and Therapeutic Monitoring.* Singapore: World Scientific.

Beauchamp, J., Kirsch, F., Buettner, A., 2010. Real-time breath gas analysis for pharmacokinetics: monitoring exhaled breath by on-line proton-transfer-reaction mass spectrometry after ingestion of eucalyptol-containing capsules. *Journal of Breath Research* 4:026006.

Farhi, L.E., 1967. Elimination of inert gas by the lung. *Respiration Physiology* 3:1-11.

Gordon, N.J., Salmond, D.J., Smith, A.F.M., 1993. A novel approach to nonlinear/non-Gaussian Bayesian state estimation. *IEE Proceedings F* 140:107-113.

Herbig, J., Müller, M., Schallhart, S., Titzmann, T., Graus, M., Hansel, A., 2009. On-line breath analysis with PTR-TOF. *Journal of Breath Research* 3:027004.

King, J., Koc, H., Unterkofler, K., Mochalski, P., Kupferthaler, A., Teschl, G., Teschl, S., Hinterhuber, H., Amann, A., 2010a. Physiological modeling of isoprene dynamics in exhaled breath. *Journal of Theoretical Biology* 267:626-637.

King, J., Kupferthaler, A., Frauscher, B., Hackner, H., Unterkofler, K., Teschl, G., Hinterhuber, H., Amann, A., Hoegl, B., 2012a. Measurement of endogenous acetone and isoprene in exhaled breath during sleep. *Physiological Measurement* 33:413-428.

King, J., Kupferthaler, A., Unterkofler, K., Koc, H., Teschl, S., Teschl, G., Miekisch, W., Schubert, J., Hinterhuber, H., Amann, A., 2009. Isoprene and acetone concentration profiles during exercise on an ergometer. *Journal of Breath Research* 3:027006.

King, J., Mochalski, P., Kupferthaler, A., Unterkofler, K., Koc, H., Filipiak, W., Teschl, S., Hinterhuber, H., Amann A., 2010b. Dynamic profiles of volatile organic compounds in exhaled breath as determined by a coupled PTR-MS/GC-MS study. *Physiological Measurement* 31:1169-1184.

King, J., Mochalski, P., Unterkofler, K., Teschl, G., Klieber, M., Stein, M., Amann, A., Baumann, M., 2012b. Breath isoprene: Muscle dystrophy patients support the concept of a pool of isoprene in the periphery of the human body. *Biochemical and Biophysical Research Communications* 423:526-530.

King., J., Unterkofler, K., Teschl, G., Teschl, S., Mochalski, P., Koc, H., Hinterhuber, H., Amann, A., 2012c. A modeling-based evaluation of isothermal rebreathing for breath gas analysis of highly soluble volatile organic compounds. *Journal of Breath Research* 6:016005.

King, J., Unterkofler, K., Teschl, G., Teschl, S., Koc, H., Hinterhuber, H., Amann, A., 2011a. A mathematical model for breath gas analysis of volatile organic compounds with special emphasis on acetone. *Journal of Mathematical Biology* 63:959-999.

King, J., Unterkofler, K., Teschl, S., Amann, A., Teschl, G., 2011b. Breath gas analysis for estimating physiological processes using anesthetic monitoring as a prototypic example. Proceedings of the *Annual International Conference of the IEEE Engineering in Medicine and Biology Society*, pp. 1001-1004, August 30 - September 3, 2011, Boston, USA.

Koc, H., King, J., Teschl, G., Unterkofler, K., Teschl, S., Mochalski, P., Hinterhuber, H., Amann, A., 2011. The role of mathematical modeling in VOC analysis using isoprene as a prototypic example. *Journal of Breath Research* 5:037102.

Lindinger, W., Hansel, A., Jordan, A., 1998. Proton-transfer-reaction mass spectrometry (PTR-MS): on-line monitoring of volatile organic compounds at pptv levels. *Chemical Society Reviews* 27:347-354.

Nakamura, M., Sanjo, Y., Ikeda, K., 1999. Predicted sevoflurane partial pressure in the brain with an uptake and distribution model comparison with the measured value in internal jugular vein blood. *Journal of Clinical Monitoring and Computing* 15:299-305.

Peifer, M., Timmer, J., 2007. Parameter estimation in ordinary differential equations for biochemical processes using the method of multiple shooting. *IET Systems Biology* 1:78-88.

Schön, T., Gustafsson, F., Nordlund, P.J., 2005. Marginalized particle filters for mixed linear/ nonlinear state-space models. *IEEE Transactions on Signal Processing* 53:2279-2289.

Schubert, R., Schwoebel, H., Mau-Moeller, A., Behrens, M., Fuchs, P., Sklorz, M., Schubert, J., Bruhn, S., Miekisch, W., 2012. Metabolic monitoring and assessment of anaerobic threshold by means of breath biomarkers. *Metabolomics*, in print (DOI: 10.1007/s11306-012-0408-6).